

1 **Automated fit quantification of tibial nail designs during**
2 **the insertion using computer 3D modelling**

3
4 **Jayani P Amarathunga¹, Michael A Schuetz^{1,2}, Prasad KVD Yarlagadda^{1,}**
5 **³, Beat Schmutz¹**

6 **Jayani P Amarathunga**

7 Institute of Health and Biomedical Innovation, Queensland University of Technology,
8 Australia

9 **Michael A Schuetz**

10 Institute of Health and Biomedical Innovation, Queensland University of Technology,
11 Australia; Trauma Services and Orthopaedics, Princess Alexandra Hospital, Australia

12 **Prasad KVD Yarlagadda**

13 Institute of Health and Biomedical Innovation, Queensland University of Technology,
14 Australia; School of Chemistry, Physics and Mechanical Engineering, Science and
15 Engineering Faculty, Queensland University of Technology, Australia

16 **Beat Schmutz**

17 Institute of Health and Biomedical Innovation, Queensland University of Technology,
18 Australia

19
20 **Corresponding author**

21 Beat Schmutz, Institute of Health and Biomedical Innovation, Queensland University of
22 Technology, 60 Musk Avenue, Kelvin Grove, QLD 4059, Australia.

23 Email: b.schmutz@qut.edu.au

29 **Abstract**

30 Intramedullary nailing is the standard fixation method for displaced diaphyseal fractures of
31 the tibia. An optimal nail design should both facilitate insertion and anatomically fit the bone
32 geometry at its final position in order to reduce the risk of stress fractures and malalignments.
33 Due to the nonexistence of suitable commercial software, we developed a software tool for
34 the automated fit assessment of nail designs. Further, we demonstrated that an optimised nail,
35 which fits better at the final position, is also easier to insert.

36 3D models of two nail designs and 20 tibiae were used. The fitting was quantified in terms of
37 surface area, maximum distance, sum of surface areas and sum of maximum distances by
38 which the nail was protruding into the cortex. The software was programmed to insert the nail
39 into the bone model and to quantify the fit at defined increment levels.

40 On average, the misfit during the insertion in terms of the four fitting parameters was smaller
41 for the ETN-Proximal-Bend (476.3mm², 1.5mm, 2029.8mm², 6.5mm) than the ETN
42 (736.7mm², 2.2mm, 2491.4mm², 8.0mm). The differences were statistically significant ($p \leq$
43 0.05). The software could be used by nail implant manufacturers for the purpose of implant
44 design validation.

45 **Keywords**

46 3D modelling, automation, tibia, intramedullary nail, nail fit, fracture fixation

47

48

49

50

51 Introduction

52 Intramedullary nailing is the standard fixation method for displaced diaphyseal fractures of
53 long bones such as tibia and femur in adults.^{1,2} The anatomically shaped modified tibial nails
54 allows an easier insertion, enhances the ‘bone-nail construct’ stability, and reduces axial mal-
55 alignments of the bone fragments as well as the risk of stress fractures.³⁻⁶

56 The nail shape validation is equally important for both newly designed nail implants and
57 modified nail designs. In the traditional approach, the nail implant validation was conducted
58 using cadaver bone trials or clinical studies. As the nail insertion takes place on the bone, the
59 geometric misfit of the nail to the bone cannot be visually assessed or quantified like in the
60 case of pre-contoured plates.⁷ It is to note that, for intramedullary nails, ease of nail insertion
61 as well as anatomical fitting of the nail to the bone at the final position are equally important
62 to reduce the risk of iatrogenic fractures in the intra-operative stage, stress fractures in the
63 post-operative stage and to avoid malalignment of bone fragments. Either, ease of nail
64 insertion or anatomical fitting of the nail to the bone at the final implanted position cannot be
65 visually assessed.

66 Traditionally, the anatomical fitting of nail designs is assessed through cadaver trials. While
67 they form an important and integral part of the validation process they suffer the following
68 drawbacks. The insertion force associated with the insertion depth of the nail can be obtained
69 by utilising an instrumented nail. Even though this load history profile can be used as an
70 indicator for the anatomical fitting of the nail design to a particular bone, it does not provide
71 any information about the locations where the mismatches occurred or the extent of mismatch
72 of the nail implant to the bone..⁸ In addition, this method cannot be used for obtaining the
73 anatomical mismatch of the nail design to the bone when the nail is at its final implanted
74 position.

75 The utilisation of x-ray images is an alternative for assessing the anatomical fit of the nail
76 design to a particular bone. However, x-rays are in the form of 2D and it does not necessarily
77 indicate the true fit between nail and the bone in 3D. Moreover, x-rays contain an unknown
78 amount of magnification and distortion which adversely affect to the accuracy of the bone-
79 nail fit quantification data.

80 The nail implant validation in the form of cadaver bone trials is also limited by the
81 availability of number of cadaver specimens.

82 Furthermore, the available collection of the cadaver specimens might not truly represents the
83 target patient population in terms of age, ethnicity as well as the stature.

84 In addition, cadaveric specimens are not suitable for assessing different nail designs with the
85 same bone, as multiple insertions and removals can compromise the structural integrity of the
86 bone.⁸

87 To address the limitations associated with traditional approach, the authors have previously
88 developed a semi-automated method utilising computer 3D models of bone and nail implants
89 for quantifying the anatomical misfit of nail designs in their final position inside 3D tibiae
90 models.⁹ The application of that method for twenty Japanese tibia models has demonstrated
91 that the modified Expert Tibial Nail (ETN Proximal Bend) fits better than the original ETN at
92 the final position. In the ideal case, after repositioning the main fragments, the bone geometry
93 should be identical to the intact bone. Therefore, intact tibiae were used in that study for
94 assessing the anatomical fit of the nail designs as this provides a more accurate indication of
95 nail fit for a particular tibia.

96 While this covers one aspect of the design validation for an intramedullary nail, the question
97 still remains whether the nail design that anatomically fits better at the final position is also

98 easier to insert. It is important to note that, the path of the nail tip during the insertion is
99 determined by both nail design and the bone geometry.

100 Wallenböck et al have conducted a quantitative study and demonstrated that the nail design
101 influences both the implantability as well as the removal of the nail.⁸ Therefore, the answer to
102 this question is of great importance to both implant manufacturers and clinicians alike.

103 The previously developed virtual method, based on manual processing utilising commercial
104 reverse-engineering software, is not suited for automating and quantifying the nail insertion
105 process.

106 Therefore the first objective of this study was to develop a customised software tool for
107 assessing the anatomical fit between bone and nail designs during the insertion process and at
108 the final position. The second aim was to determine whether the optimised ETN design,
109 which fits better at the final position, is also easier to insert. To the best of our knowledge,
110 this is the first study which presents a quantitative 3D analysis of bone-nail anatomical fit
111 during the insertion process.

112

113 **Materials and methods**

114 ***3D models of bones***

115 3D models of the medullary canals/ inner cortex surfaces of twenty Japanese tibiae were
116 available from the previous study.⁹ The morphological bone data was obtained by means of
117 CT scans and reconstructed using a commercial software (Amira, FEI, Hillsboro, OR)
118 according to a standard protocol.

119 The donors (male-6 and females -14) mean age was 64 years (, range: 44-77, SD: 10.6) and
120 the mean height was 155cm (, range: 142-178, SD: 8.4). We used right tibiae and all the bone
121 models were in the normal appearance with no reported bone deceases. The 3D models were
122 first saved in the STL-file format and then imported into Matlab (The Mathworks, Natick,
123 MA) as matrices of vertices and faces.

124

125 ***3D models of nails***

126 The 3D models of the two different nail designs (ETN (Expert Tibial Nail) and ETN-
127 proximal Bend –Synthes, Bettlach, Switzerland) were used as in the previous study.⁹ The
128 ETN proximal bend is a modified version of the original ETN. In order to improve the
129 anatomical fitting of the nail modified ETN (ETN Proximal bend) a new bend has been
130 introduced to the original ETN at the distal tip. In addition, the existing proximal bend has
131 been moved to a more proximal location.

132 The appropriate nail length for each bone model was chosen according to clinical
133 conventions. The nail diameter was chosen such that the nail sufficiently fills the medullary
134 cavity for achieving a stable bone-nail construct. The digital files were imported into the
135 reverse engineering software package Rapidform2006 (Inus Technology Inc., Seoul, Korea)
136 to extract the outer surfaces and to create polygonal meshes of the nail models as the screw
137 hole or the thread details were not needed. All 3D polygon meshes of the nails' outer surfaces
138 were then imported into Matlab as matrices of vertices and faces.

139 ***Nail entry point***

140 The nail entry point on the inner cortex surface was available for each nail and bone model
141 from the previous study. The nail entry point on the inner cortex surface has been established

142 by the authors according to the implant manufactures' guidelines¹⁰ using an anterior and a
143 sagittal view.⁹ The nail entry point was same for both nail designs (ETN and ETN Proximal
144 bend) by referring to the manufacturer's technical guidelines.

145 ***Quantification of nail fit***

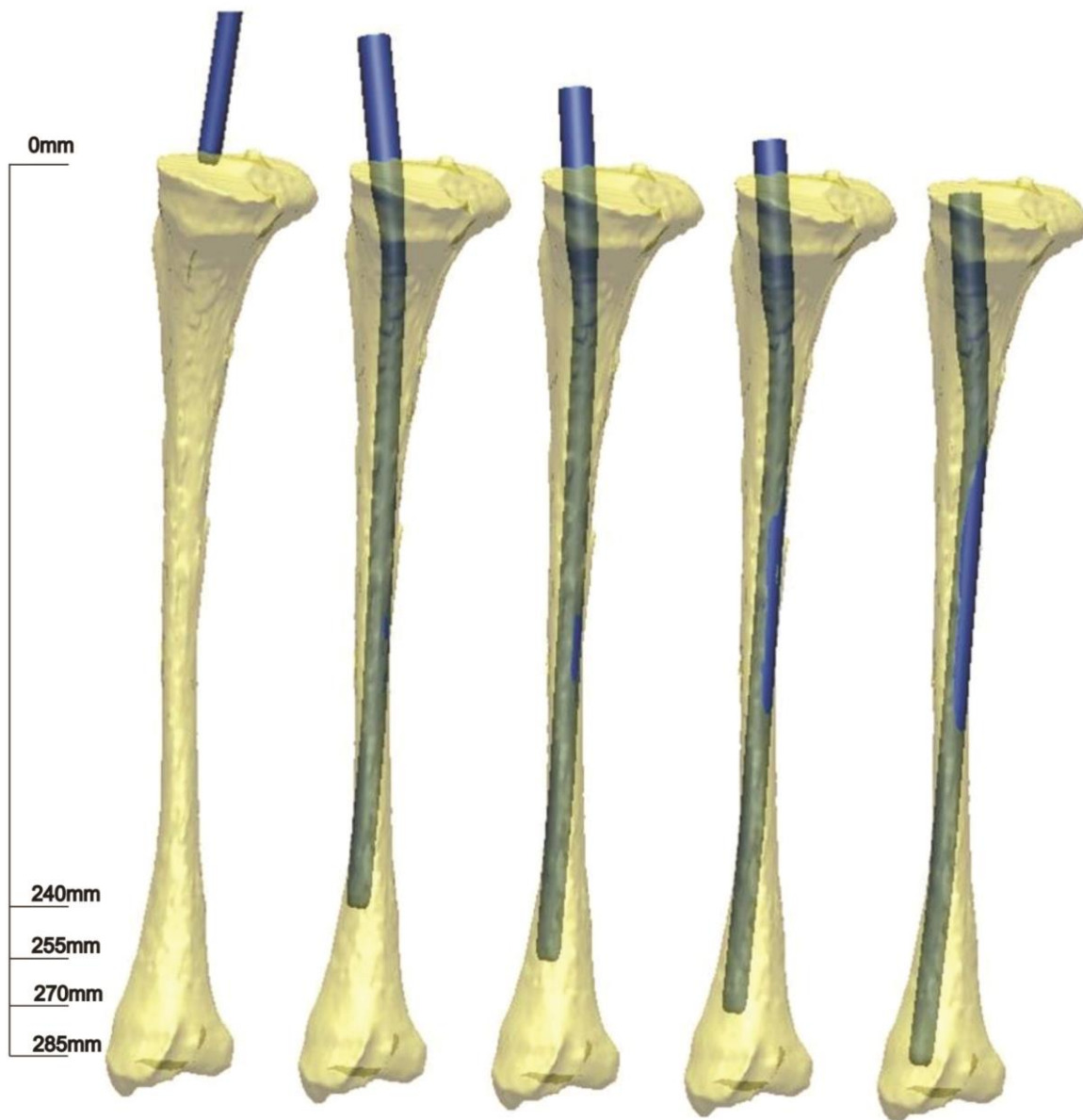
146 In an ideal case, the anatomically shaped nail fits entirely inside the medullary cavity of the
147 bone which means that the bone-nail construct stability is optimal and the axial anatomical
148 alignment of the bone is preserved. If there is a geometrical mismatch of the nail to the bone,
149 the nail model protrudes from the 3D model of the medullary canal of the intact and the
150 extent of nail protrusion indicates the amount of mismatch. Therefore, the anatomical fitting
151 of the nail model to a particular bone was quantified

152 in terms of the total surface area, and the maximum distance (in the axial plane) by which nail
153 was protruding from the medullary cavity of the virtual model.⁹ The sums of protrusions
154 (surface area and maximum distance), calculated at each increment level, were used to
155 assess/quantify the overall fitting of each design for a particular tibia model. The nail fitting
156 was quantified for the unreamed bones. The two-sided paired t-test was used to test for
157 statistical significance. The level of statistical significance was set to $p \leq 0.05$.

158 ***Development of automated fit quantification tool***

159 The methods were developed to quantitatively assess the anatomical fit of the nail during the
160 insertion and coded in Matlab software using computer programming techniques and related
161 mathematics. Starting at the entry point, the fit analysis tool was programmed to
162 automatically insert the nail model at user defined increments into the 3D model of the inner
163 cortex surface until the nail was fully inserted. For this study the anatomical fitting was
164 quantified at 15mm increments until full insertion. At each increment level, the optimal nail

165 position (with the least area of protrusion) was obtained and quantified while keeping the
166 proximal part of the nail centred at the nail's entry point on the bone model.



167

168 Figure 1: The illustration of the automated nail insertion into the inner cortex surface. The nail insertion levels
169 are set at 15mm. Left to right: The first image shows the start of the insertion, with the tip of the nail at the
entry point on the bone. The remaining images show the last 4 increment levels of the nail insertion. The nail
170 protrusion from the medullary canal is clearly visible on the posterior side of the bone for the last 3 levels.

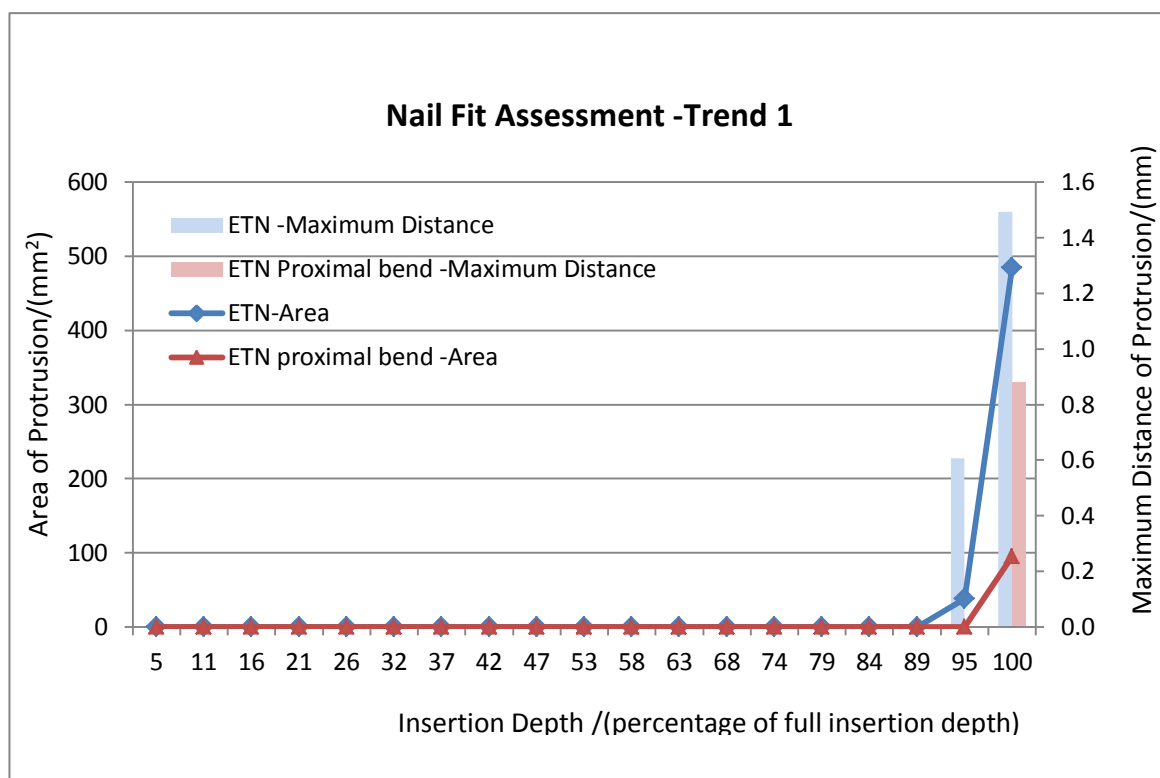
170

171 The overall misfit in terms of the sums of surface areas of nail protrusions from the medullary
172 cavity was smaller for 18 out of 20 bone models (mean: 2029.8mm², SD: 4149.2mm², range:
173 3.1-18330.2mm²) for the ETN-Proximal bend compared to the ETN (mean: 2491.4mm², SD:
174 4454.4mm², range: 197.5-20544.9mm²). Similarly, the overall misfit in terms of the sum of
175 maximum distances of nail protrusion for the ETN Proximal bend was smaller in 17 out of 20
176 bone models (mean: 6.5mm, SD: 7.5mm, range: 0.9 -34.0mm) than for the ETN (mean:
177 8.0mm, SD: 10.5mm, range: 1.1-50.7mm). The difference between the original ETN and
178 ETN Proximal bend in terms of overall misfit based on total surface area was statistically
179 significant ($\rho < 0.05$). However the differences between ETN and ETN Proximal bend in
180 terms of the overall misfit based on maximum distance of protrusion was not statistically
181 significant.

182 Similarly, the greatest misfit during the insertion in terms of the maximum area of the nail
183 protrusion for the ETN-Proximal bend was smaller for 18 out of 20 bone models (mean:
184 476.3mm², SD: 628.0mm², range: 2.0-2591.6mm²) compared to the ETN (mean:
185 736.7mm², SD: 637.0mm², range: 92.6-2822.5mm²). Also the greatest misfit in terms of the
186 maximum distance of protrusion for the ETN –Proximal bend was smaller for 18 out of 20
187 bone models (mean: 1.5mm, SD 1.0mm, range: 0.6-4.5mm) than that for the ETN (mean:
188 2.2mm, SD: 1.4mm, range: 0.6-6.7mm). The difference between the original ETN and the
189 ETN Proximal bend in terms of the greatest misfit based on both surface area and the
190 maximum distance of protrusion was also statistically significant ($\rho < 0.05$). The results are
191 summarised in Table 1.

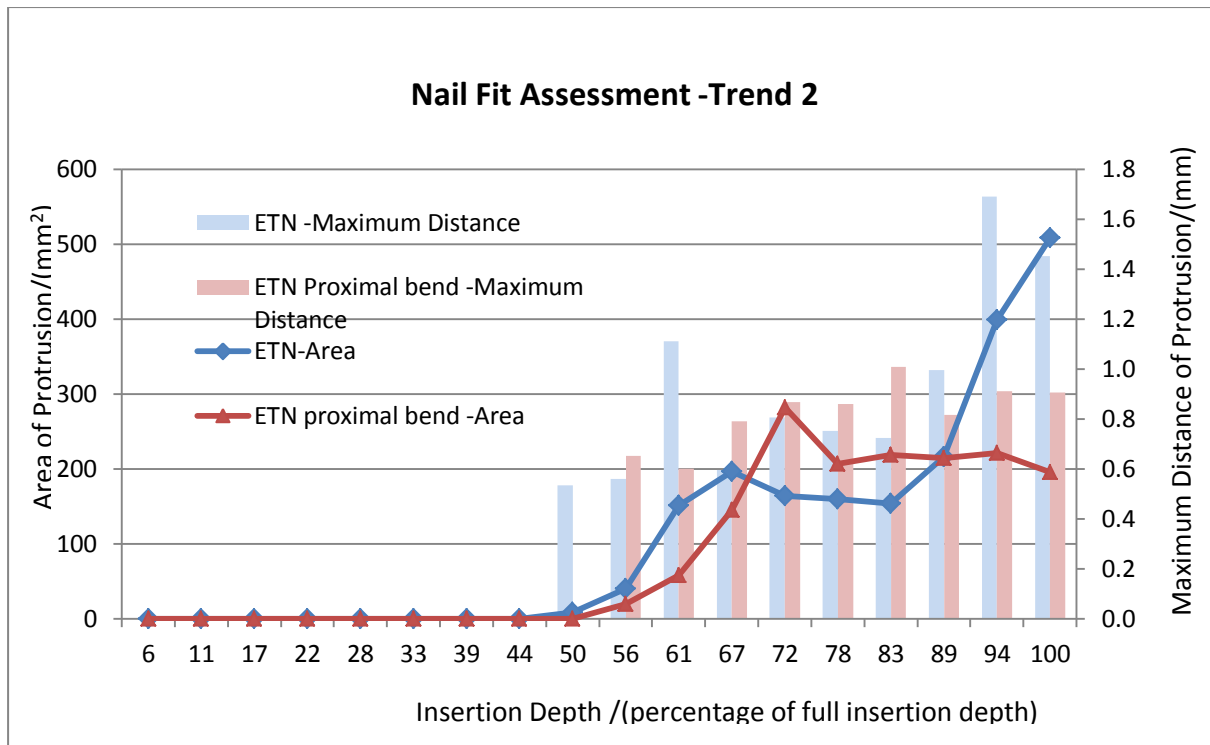
192 By plotting the area and maximum distance of the nail protrusion against the percentage nail
193 insertion depth, we were able to identify three trends of nail protrusion patterns

194 Trend 1: The area of protrusion rapidly increased at the last few levels for both nail designs.
 195 The overall misfit of the ETN Proximal bend is smaller than that of the ETN. Eight tibiae
 196 were in this category (Bone number: 2, 3, 7, 9, 13, 14, 19, and 20).



197 Please see Figure 2: The illustration of nail protrusion pattern for Trend 1. The insertion depth is presented as a %
 198 of the full nail length. The area of protrusion increased rapidly at last few levels for both nails. The overall misfit
 of ETN Proximal bend is smaller than that of ETN.

199
 200 Trend 2: The surface area of nail protrusion increased for the ETN Proximal bend after
 201 inserting the first half of the full nail length and then decreased within the last few levels
 202 compared to the ETN. However, the overall misfit based on the sums and maximum values
 203 for the area of protrusion in the ETN Proximal bend was smaller than that of the ETN when
 204 considering the whole insertion Six tibiae were in this category (Bone number: 4, 5, 6, 8, 10
 205 and 12).



206

207

Figure 3: The illustration of nail protrusion pattern for Trend 2. The insertion depth is presented as a % of the full nail length. The area of protrusion increased for ETN proximal bend after inserting the 50% of the nail length and then decreased within the last few levels compared to ETN. The overall misfit of ETN proximal bend is smaller than that of ETN.

208

209

Trend 3: The surface area of nail protrusion increased for the ETN Proximal bend after

210

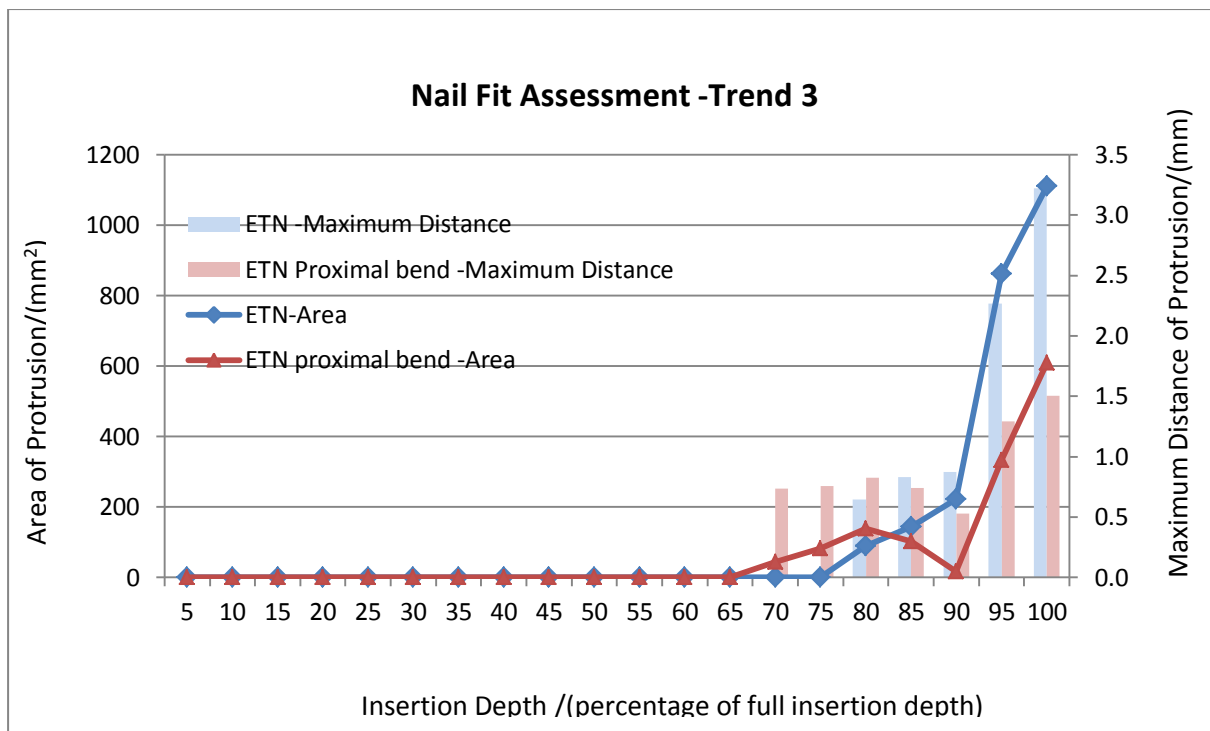
inserting the first half of the nail and then it showed a sinuous pattern. However, the overall

211

misfit of the ETN Proximal bend was smaller than that of the original ETN. Three tibiae were

212

in this category (Bone number: 11, 15 and 18).



213

214

Please see Figure 4: The illustration of nail protrusion pattern for Trend 3. The insertion depth is presented as a % of the full nail length. The surface area of protrusion increased for ETN Proximal bend after inserting the first half of the nail length and then it showed a sinuous pattern. The overall misfit of ETN proximal bend is smaller than that of ETN.

215

216

217 It is to note that three tibiae did not fall into one of these categories (Bone number: 1, 16 and

218 17). In Tibia #1, although the plot of the surface area of the nail protrusion looked like trend

219 2, the overall fitting was better for the ETN compared to the ETN Proximal bend. Tibia #16

220 has a very narrow canal and even the smallest nails (8mm diameter) started to protrude when

221 inserted 43% and 33% of the full nail length of the ETN and the ETN Proximal bend

222 respectively. In Tibia #17, the plot of the surface area of the nail protrusion looked like trend

223 3, however the overall fitting of the original ETN was better when compared to the ETN

224 Proximal bend.

225 When considering the nail fitting at the final position, the misfit of the ETN Proximal bend

226 was smaller for 19 out of 20 bone models in terms of the surface area of the nail protrusion

227 (mean: 409.0mm², SD: 603.2mm², range: 0-2591.6mm²) compared to the ETN (mean:
228 714.8mm², SD: 640.1mm², range: 24.1-2822.5mm²). Moreover, the misfit of the ETN
229 Proximal bend in terms of the maximum distance of the nail protrusion was smaller for 18 out
230 of 20 bone models (mean: 1.3mm, SD: 1.1mm, range: 0-4.46mm) compared to the ETN
231 (mean: 2.1mm, SD: 1.4mm, range: 0.6-6.7).

232 For the bone models in this study, the ETN Proximal bend can be inserted 50% of the nail's
233 full length for 19 bone models without any protrusion and by 70% on average. Similarly, the
234 ETN can be inserted 50% of its full length without any protrusion for 18 bone models and by
235 66% on average.

236 Regardless of the nail design, the majority of the nails started to protrude at the posterior side
237 of the bone (ETN: 10 out of 20 nail protrusions, ETN Proximal bend: 9 out of 18 nail
238 protrusions) during the insertion. The second main protrusion site was at the medial side of
239 the bone (ETN: 9 out of 20, ETN Proximal bend: 5 out of 20). When considering the nail
240 fitting at the final position, the majority of the nails protruded at the posterior side in the
241 middle third of the tibia (ETN: 15 out of 20 bone models, ETN Proximal bend: 11 out of 17
242 bone models) and the second main protrusion site was at the medial side of the tibia (ETN: 5
243 out of 20, ETN Proximal bend: 5 out of 20). For all the cases, during insertion, the protrusion
244 appeared in the mid or distal shaft on the bone. At the final position, the majority of
245 protrusion sites similarly appeared in the mid or distal shaft of the bone, but in two cases, the
246 protrusion site appeared in the distal part of the bone. For trend 3, both nail designs started to
247 protrude in the medial side and then it shifted to the posterior side of the bone at the final
248 position. Other than these observations, we were not able to identify a clear relationship
249 between protruding trends and the protruding side on the bone.

250 The average elapsed time for processing one pair of bone and nail models was 90 hours. For
251 protrusion trend 1 and 3, the average time elapsed for processing one pair of bone-nail
252 models was shorter (59 hours) compared to the protrusion trend 2 (106 hours), regardless of
253 the nail design. All the fit assessment tasks were executed on QUT HPC (High Performance
254 Computer Centre) group's SGI Altix XE Cluster which is composed of 1924x 64bit Intel
255 Xeon Cores.

256

257 **Discussion**

258 The optimal design of anatomically shaped nail implants enables ease of insertion and better
259 fitting at the final position. The implant shape validation is one of the most important aspect
260 of designing a new or improving an existing nail design. In traditional approach, the implant
261 shape validation is often conducted through cadaver bone trials and clinical studies based on
262 planar x-ray images.

263 To address the limitations of the traditional approach, the authors have previously developed
264 a virtual method for quantitatively assessing the anatomical fit of the nail designs in their
265 final position inside 3D tibia models utilising a reverse engineering software.⁹ Although the
266 previous study covers one aspect of validation of nail designs, it does not provide any
267 indication whether the nail design which fits better at the final position is also easier to insert.
268 In addition, the previous method utilising commercial software is not capable for of assessing
269 the anatomical fit between nail and bone during insertion.

270 Therefore, in this study, we addressed the main limitations of the previously developed
271 virtual method. To the best of our knowledge this is the first customised software tool which
272 quantifies the geometric misfit between the nail designs and tibiae during the insertion as well

273 as at the final position. In an ideal case, after repositioning the main fragments, we expect to
274 achieve the original anatomical shape of the bone. In other words, if the nail shape fits better
275 to an intact bone, it is more likely to ensure/allow anatomical alignment of main fragments.
276 Therefore we used intact tibiae to assess anatomical fitting of the two nail designs as they
277 provide the most accurate indication of any geometric mismatch between bone and nail. Egol
278 et al¹¹ argued that any mismatch in the curvature between the nail and bone can be
279 accommodated by angulation at the fracture and overreaming. However, for proximal or
280 distal shaft fractures, there are cases where a mismatch between bone and nail geometry
281 cannot be eliminated through angulation of the main fragments. It is to note, if the fracture
282 accommodates any large mismatch between bone and nail, then the resulting alignment of
283 main fragments may not be within the clinically acceptable range. Further, a biomechanical
284 study confirmed that overreaming will result in weakening of the bone which may cause
285 iatrogenic fractures and/or post-operative stress-fractures.¹²

286 Based on the results obtained, the ETN Proximal bend shows a statistically significant better
287 anatomical intramedullary fit with least nail protrusion than the original ETN during the
288 insertion as well as at the final position. The overall misfit in terms of surface area of
289 protrusion is smaller for ETN Proximal bend (average: 2029.8mm²) when compared to the
290 original ETN (average: 2491.4mm²). Similarly, the overall misfit in terms of maximum
291 distance of protrusion is also smaller for ETN Proximal bend (average: 6.5mm) when
292 compared the original ETN (average: 8.0mm). The greatest misfit during the insertion in
293 terms of both surface area and maximum distance of protrusion is also smaller for the ETN
294 Proximal bend (average: 476.3mm² and 1.5mm respectively) than that of the original ETN
295 (average: 736.7mm², 2.2mm respectively). The average length by which the nail can be
296 inserted into the bone without any protrusion is 70% of the nails' full length for the ETN

297 Proximal bend while it is 66% for the original ETN. This suggests that, if at all, stress
298 fractures are more likely to occur during the insertion of the second half of the nail.

299 The results for the nail fitting at the final position clearly shows that the ETN proximal bend
300 fits better at the final position in terms of both surface area and the maximum distance of
301 protrusion (average: 409.0mm², 1.3mm respectively) when compared to the original ETN
302 (average: 714.8mm², 2.1mm).

303 To the best of our knowledge, this is the first study which demonstrates that an optimised
304 tibial nail design which fits better at the final position is indeed also easier to insert.
305 Furthermore, the software tool was developed to function independent of bone and nail
306 geometry. Therefore it will be suitable for quantifying the anatomical fitting of other nails
307 such as femoral nails and humeral nails with only minor modifications and/or extensions of
308 the software code.

309 A further advantage of the developed software tool is that the different nail designs can be
310 assessed by inserting into the same bone model without damaging the bone, or compromising
311 its structural integrity through the multiple insertions and removals of a nail.. In addition, the
312 customised software tool is designed for quantifying the nail fitting at user defined increment
313 levels which enables detailed investigation in the proximity of the misfits.

314

315 Moreover, if morphological bone data is obtained by means of MRI instead of CT, the
316 presented method will be no-radiation as well as non-invasive. Therefore, it is suitable
317 acquiring the bone data from healthy donors to reconstruct the 3D bone models. Then, the
318 developed software tool can be effectively used for the nail fit quantification during the
319 insertion in a particular target population.

320 The long execution time (average: 90 hours) can be considered as the main limitation of the
321 developed customised software tool and is subject of further research by our group. The
322 current standard methods for reconstructing bone models from CT or MRI data also take a
323 long time. The improved fit quantification software with reduced execution time would need
324 to be also incorporated with a time saving method of bone 3D reconstruction in order to
325 ensure the benefits of the presented method as a pre-operative planning tool in clinics.
326 Furthermore, the developed software tool quantifies only the geometric misfit between bone
327 and nail designs using the two fit quantification parameters (total surface area and the
328 maximum distance of protrusion). As such, the measurements obtained do not yet provide
329 any information regarding the deformation of nail and bone during the insertion process and
330 whether a certain amount of misfit can be tolerated, or might result in fracture extension or
331 even lead to a stress fracture in the bone. Therefore the extension of the present work will be
332 the incorporation of finite element analysis (FEA) into the fit assessment, which will enable
333 the quantification of forces exerted on the cortex through a specific nail design during
334 insertion and/or removal of the nail. The authors are currently working on a project aiming to
335 address this. Even though, the developed software tool mainly facilitates implant shape
336 validation, it could potentially be useful in pre-operative planning assisting the surgeon to
337 choose the most appropriate nail design for the bone geometry of a particular patient. The
338 developed method will facilitate the achievement of full recovery and hence improvement in
339 patients quality of life through the anatomic reduction.

340

341 **Acknowledgements**

342 David Warner (High Performance Computer centre (HPC), Queensland University of
343 Technology) assisted with advanced software coding.

344 Funding Acknowledgement

345 None

346 Conflict of Interest

347 Dr. Beat Schmutz has received an industrial scholarship from Synthes GmbH

348

349 References

- 350 1. Lefavre KA, Guy P, Chan H and Blachut P. Long-Term Follow-up of Tibial Shaft Fractures
351 Treated With Intramedullary Nailing. *Journal of Orthopaedic Trauma* 2008; 22: 525-9.
- 352 2. Penzkofer R, Maier M, Nolte A, Oldenburg GV, Püschel K, Bühren V and Augat P. Influence of
353 Intramedullary Nail Diameter and Locking Mode on the Stability of Tibial Shaft Fracture Fixation.
354 *Archives of Orthopaedic and Trauma Surgery* 2009; 129: 525-31.
- 355 3. Henley MB, Meier M and Tencer AF. Influences of Some Design Parameters on the
356 Biomechanics of the Unreamed Tibial Intramedullary Nail. *Journal of Orthopaedic Trauma* 1993; 7:
357 311-9.
- 358 4. Nork SE, Barei DP, Schildhauer TA, Agel J, Holt SK, Schrick JL and Sangeorzan BJ.
359 Intramedullary Nailing of Proximal Quarter Tibial Fractures. *Journal of Orthopaedic Trauma* 2006; 20:
360 523-8.
- 361 5. Kuhn S, Hansen M and Rommens P. Extending the Indications of Intramedullary Nailing with
362 the Expert Tibial Nail. *Acta Chirurgiae Orthopaedicae et Traumatologiae Cechoslovaca* 2008; 75: 77-
363 87.
- 364 6. Kuhn S, Hansen M and Rommens PM. Extending the Indication of Intramedullary Nailing of
365 Tibial Fractures. *European Journal of Trauma and Emergency Surgery* 2007; 33: 159-69.
- 366 7. Goyal KS, Skalak AS, Marcus RE, Vallier HA and Cooperman DR. Analysis of Anatomic
367 Periarticular Tibial Plate Fit on Normal Adults. *Clinical Orthopaedics & Related Research* 2007; 461:
368 245-57.
- 369 8. Wallenbock E and Koch G. Knick oder Krümmung beim unaufgebohrten Tibiamar-knagel:
370 Experimentelle Studie. *Langenbecks Archiv für Chirurgie* 1997; 382: 257-65.
- 371 9. Schmutz B, Rathnayaka K, Wullschlegler ME, Meek J and Schuetz MA. Quantitative Fit
372 Assessment of Tibial Nail Designs using 3D Computer Modelling. *Injury* 2010; 41: 216-9.
- 373 10. Synthes: Expert tibial Nail:Technique Guide Synthes GmbH. 2006.
- 374 11. Egol KA, Chang EY, Cvitkovic J, Kummer FJ and Koval KJ. Mismatch of Current Intramedullary
375 Nails With the Anterior Bow of the Femur. *Journal of Orthopaedic Trauma* 2004; 18: 410-5.
- 376 12. Pratt DJ, Papagiannopoulos G, Rees PH and Quinnell R. The effects of medullary reaming on
377 the torsional strength of the femur. *Injury* 1987 5//; 18: 177-9.

378

379